

# CT angiography of the celiac trunk: anatomy, variants and pathologic findings

Nilgün Işıksalan Özbulbul

## ABSTRACT

Celiac trunk variants and pathologies are relatively common occurrences. With the advent of computed tomography (CT) technology, these conditions are being diagnosed with an increased frequency even among asymptomatic patients. CT angiography is used noninvasively for preoperative staging and vascular mapping in patients with pancreatic and hepatobiliary neoplasm. Multidetector-row CT (MDCT) also allows the accurate depiction of the abdominal splanchnic vessels for stenosis, collateral vessels and atherosclerotic plaques. In this study, we describe the normal anatomy and variants of the celiac trunk as well as associated pathologic conditions, such as stenosis, occlusion, aneurysm and median arcuate ligament compression syndrome. The overall aim of this study was to emphasize the clinical importance of these abnormalities.

**Key words:** • celiac artery • computed tomography  
• CT angiography

**B**ecause of the development of interventional techniques to manage hepatic tumors and liver transplantation, the accurate depiction and definition of the celiac trunk and its branches have important clinical implications. With the recent advent of CT technology, multidetector-row CT (MDCT) has become a valuable tool for the visualization of the celiac trunk and its branches. Moreover, reformatting three-dimensional MDCT images allow detailed visualization of the complex vascular anatomy. Therefore, small vessel abnormalities may be detected with greater frequency in symptomatic and asymptomatic patients using these techniques.

The aim of the present study was to illustrate the normal anatomy and variants of the celiac trunk as well as associated pathologic conditions, such as stenosis, occlusion, aneurysm and median arcuate ligament compression syndrome.

## Materials and methods

We retrospectively reviewed our archives for celiac trunk pathologies in patients who had undergone abdominal MDCT angiography examination. All of the patients had undergone CT angiography for the abdominal aorta and its branches using 16- or 64-row CT units (Lightspeed 16, GE Medical Systems, Milwaukee, Wisconsin, USA; or Aquilion 64, Toshiba Medical Systems, Tokyo, Japan). Because the accompanying pathologies of the celiac trunk and its branches can cause some abnormalities associated with other mesenteric vessels, we usually include the superior and inferior mesenteric artery in the scanning area. Consequently, the area from the level of the diaphragm to the iliac bifurcation is scanned. The scanning parameters are as follows: detector configuration of 16 x 0.625 mm or 64 x 0.5 mm; 120 kVp; 120–170 mAs; pitch of 1.3–1.5; and gantry rotation time 500 ms or 350 ms. We do not routinely use water as the oral contrast material to distend the stomach and proximal small bowel. We use an 18 G IV line in the antecubital vein and the same contrast material injection protocol independently of the CT scanner used. Approximately 100–110 mL of nonionic contrast material (350 mgI/mL) is injected with an automatic double-head power injector at a flow rate of 4 mL/s.

In the 64-slice CT scanner, the scan delay is set using automated bolus-tracking software (SureStart, Toshiba Medical Systems) to capture 150 HU of the abdominal aorta at the level of the celiac trunk. In the 16-slice CT scanner, the scan delay is set manually using semi-automated bolus-tracking software (Smartprep, GE Medical Systems) to capture 100 HU of the abdominal aorta at the level of the celiac trunk. Both 3-mm and 1-mm thick images are reconstructed on both the 16- and 64-slice CT scanners and then transferred to dedicated workstations (AW 4.2, GE Medical Systems; or Vitrea 4.1.2, Toshiba Medical Systems) to build mul-

From the Department of Radiology (✉ nilgunisiksal@yahoo.com), Türkiye Yüksek İhtisas Hospital, Department of Radiology, Ankara, Turkey.

Received 4 January 2010; revision requested 12 February 2010; revision received 22 February 2010; accepted 4 April 2010.

Published online 6 August 2010  
DOI 10.4261/1305-3825.DIR.3283-10.1

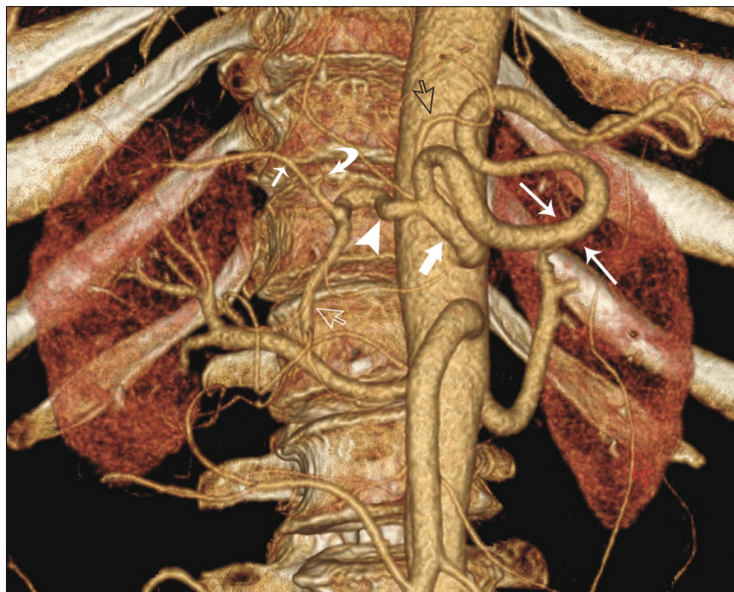


**Figure 1.** Conventional hepatic arterial anatomy in a 48-year-old man. Volume-rendered three-dimensional image created from CT angiography data showing the conventional visceral anatomy. The celiac axis (thick solid arrow) trifurcates into the splenic artery (long arrows), common hepatic artery (arrowhead) and left gastric artery (open black arrow). The common hepatic artery bifurcates into the gastroduodenal artery (open white arrow) and the proper hepatic artery. The proper hepatic artery bifurcates into the right (small arrow) and left hepatic arteries (curved arrow).

planar reformatted (MPR) and volume rendered images. The images are evaluated using three-dimensional imaging with combined maximum intensity projection (MIP) and volume rendering (VR) techniques. Because the celiac trunk and its origin are clearly visible on the sagittal plane, we prefer the sagittal plane to review these vessels.

With MDCT scanners, the ability to rapidly scan large volumes tends to cause the operator to increase the volume along the z-axis (1). As the total radiation dose delivered is directly proportional to the scan range, precise adjustment of the scan coverage is important for optimization of the dose length product (DLP) (1). Therefore, z-coverage should be adapted to the clinical indication and to possible alternative diagnoses. In general, CT dose can be decreased despite a constant image quality when using newer generations of MDCT scanners. The automatic exposure control device, which is available for modern equipment, also reduces the tube current in thin patients and increases it in overweight patients, thereby tending to maintain the image quality (1). However, if the same settings for adults are used in children, this results in a two-fold to four-fold higher dose. Therefore, low kV settings

(80 kV) and adaptation of the mAs to the weight of the child are required (1, 2). The protection of non-scanned organs is also essential in the pediatric population. In pediatric groups, the contrast injection rate is determined by the size of the cannula with the following parameters: the maximum flow rates for automated injection are 2 mL/s with a 22 G catheter, 2.5 mL/s using a 20 G catheter and 3.0–3.5 mL/s with 18 G access (2). The total amount of contrast material is calculated according to the weight of the child (2.0 mL/kg) (2).

#### Normal celiac trunk anatomy and variants

Celiac trunk anatomical variants are not infrequent, and a priori knowledge of any existing abnormalities is becoming mandatory in planning surgical and interventional procedures, especially in patients with pancreatic and



**Figure 2.** A 49-year-old woman with a replaced right hepatic artery from the superior mesenteric artery (SMA). Volume-rendered three-dimensional image created from CT angiography data showing the right hepatic artery (arrowheads) originating from SMA (black arrow). Note the celiac artery trifurcating into the left gastric artery (open black arrow), splenic artery (long arrow) and common hepatic artery. The common hepatic artery bifurcates into the left hepatic artery (curved arrow) and gastroduodenal artery (open white arrow).

hepatobiliary malignancies. According to conventional visceral anatomy, the celiac trunk originates from the abdominal aorta and gives origin to the left gastric artery, the splenic artery, and the common hepatic artery (Fig. 1). The common hepatic artery extends anteriorly and bifurcates into the gastroduodenal artery and the proper hepatic artery. The proper hepatic artery extends cephalad, runs to the left side of the common hepatic duct and then bifurcates into the right and left hepatic arteries typically immediately below the bifurcation of the common hepatic duct. Variant hepatic and celiac arterial anomalies have been reported in 55% of patients based on initial cadaveric dissections by Michels (3). According to Michels' classification, the most common variant is a replaced right hepatic artery originating from the superior mesenteric artery (Fig. 2). It is important to recognize a replaced

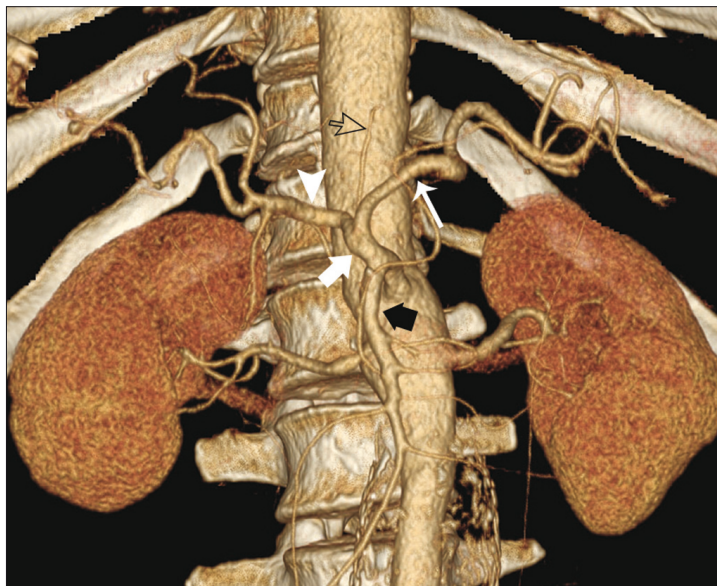


**Figure 3.** A 61-year-old man with a common trunk of the celiac axis and the superior mesenteric artery (SMA). Volume-rendered three-dimensional image created from CT angiography data showing the celiac axis (thick solid arrow) and SMA (black arrow) originating from the abdominal aorta as a single trunk. The splenic artery (long arrow) and the common hepatic artery (arrowhead) originate from the celiac axis. The left gastric artery (open black arrow) arises from the aorta.

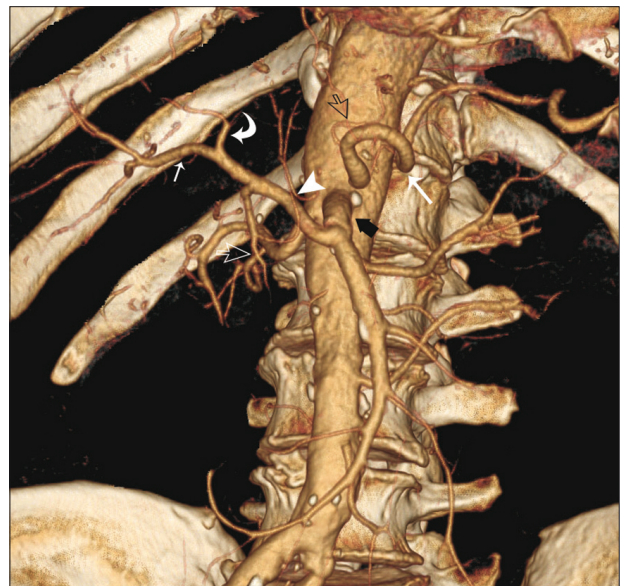


**Figure 4.** A 57-year-old man with a variation in the origin of the common hepatic artery. Volume-rendered three-dimensional image created from CT angiography data showing the common hepatic artery (arrowhead) originating from the superior mesenteric artery (SMA) (black arrow). The common hepatic artery bifurcates into the gastroduodenal artery (open white arrow) and the proper hepatic artery. The right hepatic artery (small arrow) and the left hepatic artery (curved arrow) originate from the proper hepatic artery. Note the left gastric artery (open black arrow) originating from the splenic artery (long arrow).

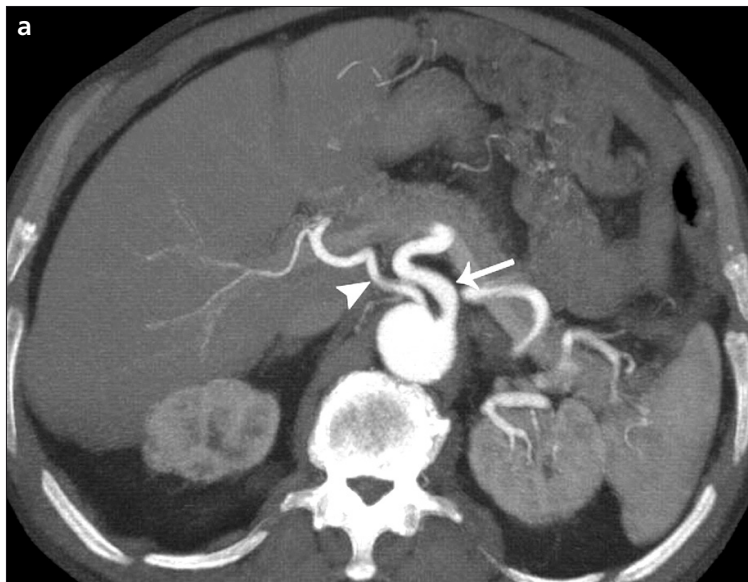
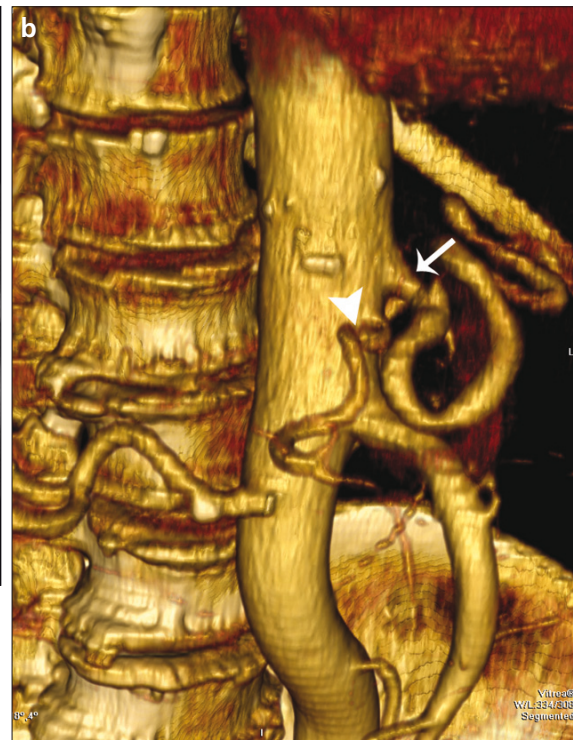


**Figure 5. a, b.** A 46-year-old woman with separate origins of common hepatic and splenic arteries. Thick-slab maximum intensity projection (MIP) axial (a) and volume-rendered three-dimensional images (b) created from CT angiography data showing separate origins of the common hepatic (arrowhead) and splenic arteries (long arrow) from the aorta. The left gastric artery originates from common hepatic artery (not shown).



right hepatic artery when performing pancreaticoduodenectomy and for porta hepatitis dissection during hepatic resection. In contrast, the right hepatic artery usually courses anterior to

the right portal vein, and the replaced right hepatic artery originates from the SMA, which courses posterior to the main portal vein in the portacaval space. MDCT angiography has a report-

ed accuracy of 97% to 98% compared with conventional angiography for the detection of arterial variants (Figs. 3–6) (4, 5). The preoperative knowledge of these variants has tremendous surgical



**Figure 6.** A 65-year-old man with a replaced right hepatic artery from the aorta. Volume-rendered three-dimensional image created from CT angiography data showing the right hepatic artery (arrowheads) originating from the aorta. The long arrow indicates the splenic artery; open black arrow, left gastric artery; curved arrow, left hepatic artery; open white arrow, gastroduodenal artery; black arrow, superior mesenteric artery.

significance when laparoscopic procedures or liver surgery are planned due to limited vision of the surgical field. Moreover, recognition of the aberrant vessels can also be useful in transcatheter arterial chemoembolization and radioembolization.

#### Median arcuate ligament syndrome

The median arcuate ligament (MAL) is a tendinous band that connects the medial borders of the crura of the diaphragm on either side of the aortic hiatus, posterior and superior to the origin of the celiac axis. A low insertion of the MAL or a high origin of the celiac or renal artery may cause extrinsic compression of the celiac, mesenteric and renal arteries from their anterior borders by this ligament (6). The etiology of this compression is not clear. However, it is thought to be due in part to the variable migration of the celiac trunk origin during embryogenesis. Thony et al. (7) have suggested that these compressions are not congenital but may be favored by changes in the relationships between the aorta and musculoskeletal structures over time. Most celiac compressions present with no symptoms due to the rich collaterals between the superior mesenteric artery and the celiac artery. Color Doppler sonography has been used as a noninvasive technique to document increases in flow velocities during end expiration. The increased flow velocity during deep expiration is known as the "Doppler duplex sign of celiac artery compression syndrome" (8). The MAL itself and its relation to the celiac artery can be shown accurately and non-

invasively with multiplanar images and three-dimensional angiograms on MDCT; therefore, this technique seems to be the most appropriate modality to diagnose MAL syndrome. Catheter angiography can suggest the diagnosis of compression to a variable degree in 10% to 50% of patients, but the MAL cannot be visualized using this technique. The diagnostic criteria for extrinsic compression of the diaphragm by the MAL are the direct visualization of the MAL on MDCT and detection of the characteristic superior notch formation on celiac angiograms. The degree of stenotic changes on celiac artery angiograms has been shown to increase with expiration and decrease or disappear with inspiration. Sagittal MPR or three-dimensional images reveal focal narrowing and acute downward angulation of the proximal portions of the celiac axis. When a hooked appearance due to the kinking (especially in the proximal portion of the celiac artery) and indentation of the adjacent aortic border are observed, they can be used as criteria to distinguish this entity from atherosclerotic stenosis (Fig. 7) (6, 9).

#### Celiac trunk aneurysm

Celiac trunk aneurysms represent a rare form of aneurismal disease that accounts for 4% of all splanchnic aneurysms (10). Moreover, the incidence of associated aneurysms is significant. Approximately 20% of patients will have an associated aneurysm, and 38% will have a second splanchnic artery aneurysm (11). Celiac artery aneurysms typically occur in the sixth decade

of life. The most common etiological cause is atherosclerosis; however, other causes include infection, tuberculosis or syphilis, trauma, fibromuscular dysplasia and polyarteritis nodosa. The majority of patients who proceed to diagnosis are symptomatic. The most common symptom is abdominal pain. Aneurysm rupture remains the major complication, and in most cases, they rupture into the peritoneal cavity. The rupture of celiac artery aneurysms into the gastrointestinal tract presents with hematemesis and bright red blood from the rectum. However, with recent advances in noninvasive imaging techniques, more cases are being detected prior to rupture. Rupture is difficult to predict and nearly always fatal when it occurs. Other documented complications include thromboembolic events. The exact presentation depends on the degree of involvement of the branched vessels of the celiac artery. Catheter angiography has been the traditional means of diagnosis. However, three-dimensional imaging with MDCT, which permits visualization of the aorta and its branches, may detect aneurysms with greater frequency in symptomatic and asymptomatic patients (Fig. 8) (10–13). Elective repair of a detected celiac artery aneurysm decreases the mortality rate to 5%. Celiac artery aneurysms can be treated either surgically by revascularization or arterial ligation, or by endovascular interventional radiology techniques. Surgical repair is indicated for symptomatic aneurysms (i.e., aneurysms larger than 3 cm) or for patients in whom the aneurysm is enlarging rapidly (10).

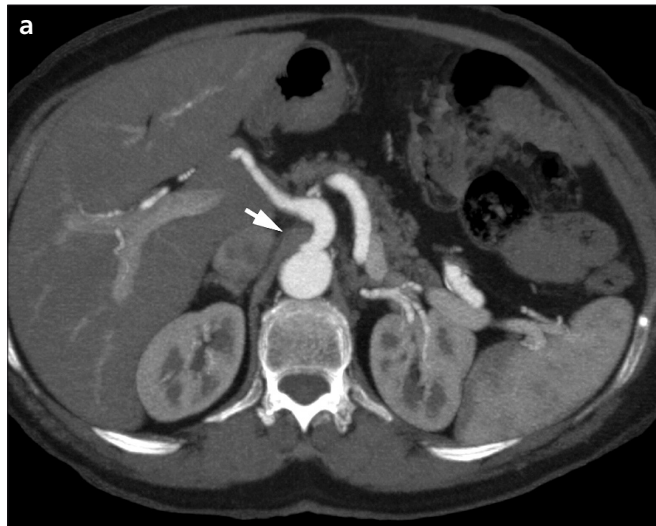


**Figure 7.** a–c. A 49-year-old man with median arcuate ligament (MAL) compression. Thick-slab maximum intensity projection (MIP) axial image (a) revealing the area surrounding the celiac axis origin representing the thickened MAL (arrow); sagittal multiplanar reformatted image (b) showing the MAL (arrows) compressing the proximal celiac artery; and volume-rendered three-dimensional (c) image created from CT angiography data showing the classical hooked appearance of the celiac artery (short arrow). The origin of the SMA is obscured by the splenic artery (long arrow).

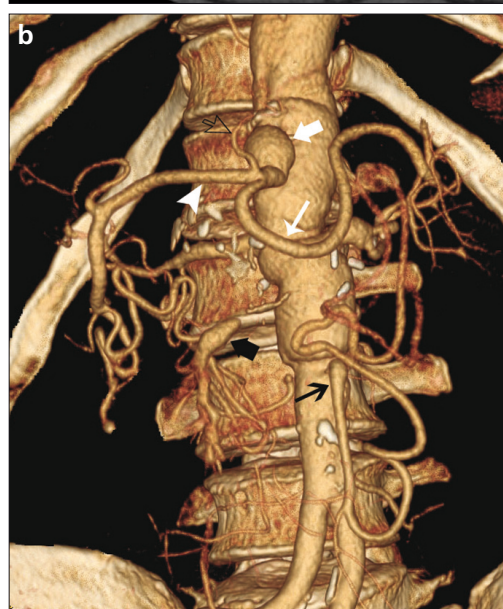


**Figure 8.** a, b. A 72-year-old man with celiac artery aneurysm. Thick-slab maximum intensity projection (MIP) axial image (a) revealing celiac artery aneurysm (thick white arrow) and trifurcation (common hepatic artery, arrowhead; splenic artery, thin white arrow). Volume-rendered three-dimensional image (b) created from CT angiography data clearly depicting the relationship of the aneurysm with the celiac arterial branches. The origin of the superior mesenteric artery (SMA) is not visible due to occlusion. The distal portion of the SMA (thick black arrow) is filled by retrograde collateral flow via the pancreaticoduodenal arcade. Note the enlarged inferior mesenteric artery (thin black arrow).

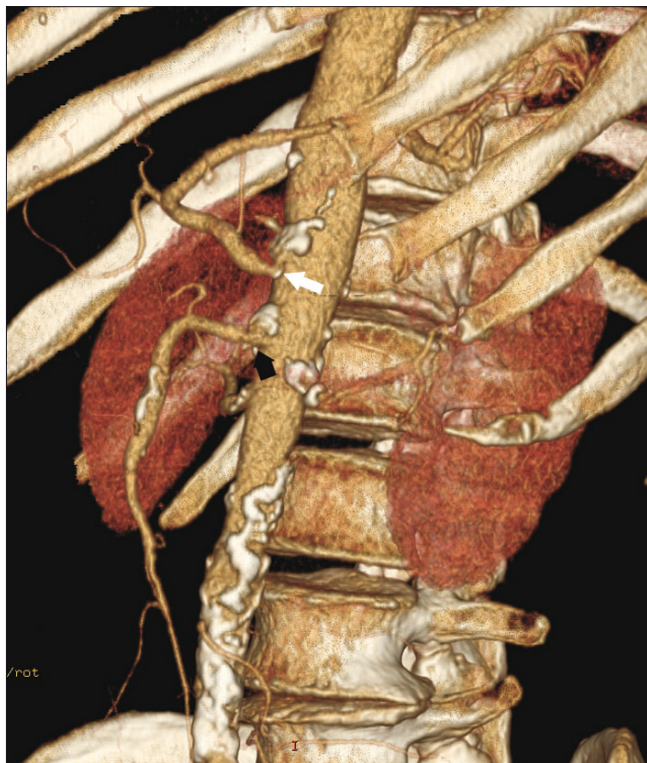


**Figure 9.** A 68-year-old man with celiac artery stenosis due to atherosclerosis. Volume-rendered left anterior oblique three-dimensional image created from CT angiography data showing significant stenosis of the celiac artery (white arrow) with calcified plaques and a concomitant finding of non-significant stenosis of the superior mesenteric artery (black arrow).

#### Celiac artery stenosis and occlusion

The suggested causes of celiac trunk stenosis are atherosclerosis, acute and chronic dissection, and compression of the celiac axis by the MAL (Fig. 9) (14, 15). Pancreatitis and pancreatic tumors have also been reported as etiologic factors of celiac trunk stenosis or occlusion (9, 14). Furthermore, ethnicity plays a role in the incidence of these different etiologies; for example, in Western populations, arteriosclerosis is reportedly the most common cause of celiac stenosis (9). Bron and Redman (16) noted an incidence of 12.5% among 713 patients referred for abdominal aortography. One percent of abdominal arteriograms detected severe stenosis of the celiac axis. The most common and important collateral vessels from the SMA in patients with celiac axis stenosis are the pancreaticoduodenal arcades and the dorsal pancreatic artery. Severe stenosis of the celiac artery is commonly associated with enlargement of the arteries of the pancreaticoduodenal arcade. It is presumed that chronic increased blood flow and turbulence through the pancreaticoduodenal ar-

cade weakens the arterial wall, which causes dilatation and tortuosity that ultimately leads to aneurysm formation (9, 15, 17). In the past, celiac axis stenosis has been cited as a reason for exclusion as a living liver transplant donor. Akamatsu et al. showed that donor hepatectomy could be safely performed in the presence of significant celiac artery stenosis (18).

In hepatic chemoembolization, celiac axis stenosis increases the risk of inadvertent splenic infarction due to the reversed blood flow in the common hepatic or left hepatic artery. Some authors have presented their clinical results using transcatheter arterial chemoembolization (TACE) procedures performed via the inferior pancreaticoduodenal arcade and the occluded celiac axis. They concluded that TACE from the arteries in front of the confluence with the proper hepatic artery seemed to be acceptable in cases of hypervascular hepatocellular carcinoma, which failed to be superselectively catheterized (19).

However, clinically significant ischemic bowel disease secondary to celiac axis stenosis is rarely encoun-

tered, mainly due to the development of rich collateral vessels from the superior mesenteric artery. In general, all three vascular axes are variably occluded or stenotic in chronic mesenteric ischemia (Figs. 10 and 11). Because of the extensive collateral vessels between the vascular territories of the three main splanchnic arteries, abdominal angina tends to occur whenever at least two of the three vessels are obstructed. The vessel lumen and stenosis are well depicted by MDCT. Thus, a clear diagnosis of atherosclerotic changes in the aorta and obstructing atheroma at the celiac axis with or without calcification can be achieved. After intervention, MDCT can be used as a noninvasive follow-up procedure to identify restenosis (17).

Celiac artery occlusion is a common finding in older adults, and stenosis is present in up to 10% of patients undergoing pancreaticoduodenectomy. Pancreaticoduodenectomy for cancers of the head of the pancreas involves division of the gastroduodenal artery. Moreover, celiac axis stenosis or occlusion can lead to fatal hepatic ischemia after pancreaticoduodenectomy unless a simultaneous revascularization of the celiac circulation is performed (20).

Isolated dissections of the mesenteric arteries are rare (21). Patients typically present with vague abdominal pain, and therefore, CT is often the first imaging modality used to identify the presence of a dissection. MDCT and three-dimensional imaging can define the dissection and assist in treatment planning (Fig. 12) (21).

#### Conclusion

We have described several pathologic conditions of the celiac trunk, as well as its normal anatomy and common variants. In the past, patients with suspected vascular disease required conventional angiography. However, MDCT angiography has become the primary tool for the evaluation of patients with suspected abnormalities of abdominal vessels. The celiac artery and its branches can be easily identified on MDCT examinations. In addition, three-dimensional and multiplanar imaging offer detailed non-invasive analyses of the celiac trunk and its branches. Overall, the benefits of MDCT can aid radiologists in planning for surgeries and other clinical interventions.

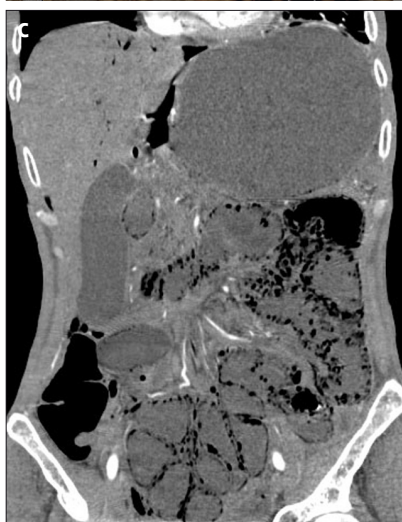
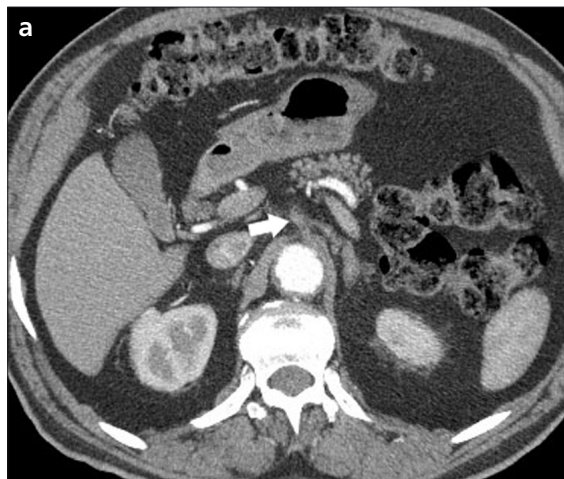
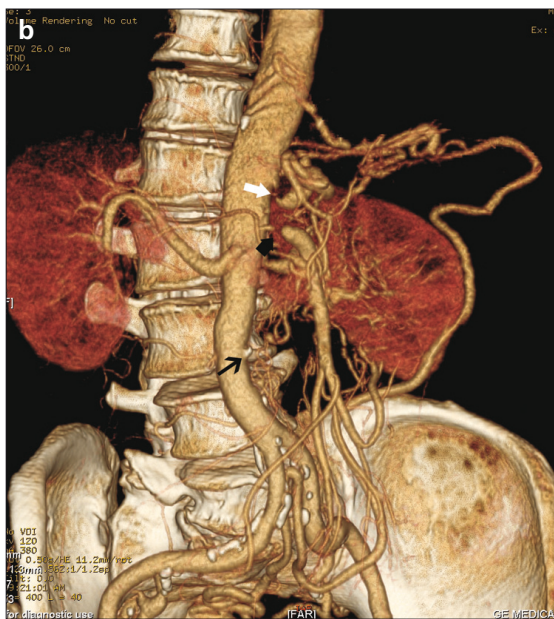
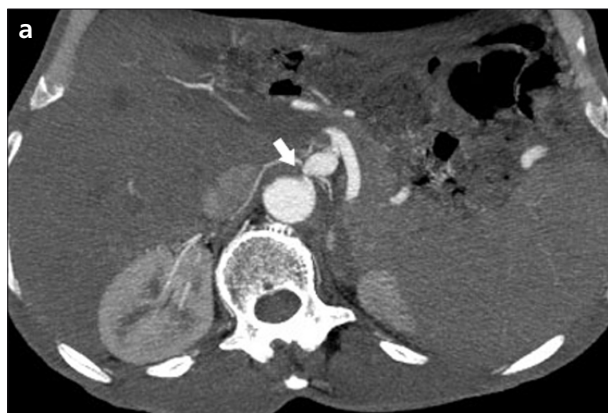


**Figure 10.** a–c. A 58-year-old man with significant stenosis of the celiac and superior mesenteric arteries. Thick-slab maximum intensity projection (MIP) axial images (a) showing significant stenosis of the celiac artery (white arrow). Volume-rendered three-dimensional image (b) created from CT angiography data clearly confirming significant stenosis of the celiac artery (white arrow) and SMA (thick black arrow). Note the total occlusion of the inferior mesenteric artery (thin black arrow). An extensive collateral network can be seen. Coronal multiplanar reformatted image (c) revealing gas in the portal vein branches and in the bowel walls. Note also the bowel dilatation.

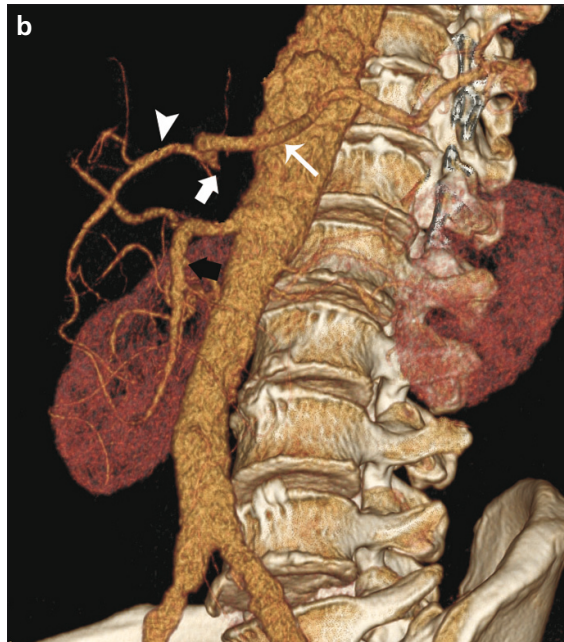


**Figure 11.** a, b. A 63-year-old man with celiac artery occlusion due to atherosclerosis. Thick-slab maximum intensity projection (MIP) axial (a) image showing total occlusion of the celiac artery (arrow). Note the diffuse atherosclerotic changes in the abdominal aorta. Volume-rendered three-dimensional image (b) created from CT angiography data revealing occlusion of the celiac artery (thick arrow). The long arrow indicates the splenic artery; arrowhead, common hepatic artery; black arrow, superior mesenteric artery.

**Figure 12.** A 59-year-old man with aortic dissection extending to the origin of the celiac artery. Thick-slab maximum intensity projection (MIP) axial image showing the aortic dissection extending to the origin of the celiac artery (arrow). Note the celiac artery originating from the true lumen.

## References

1. Stamm G. Collective radiation dose from MDCT: critical review of surveys studies. In: Tack D, Gevenois PA, ed. Radiation dose from adult and pediatric multidetector computed tomography. Berlin: Springer, 2007; 81–97.
2. Yekeler E. Pediatric abdominal applications of multidetector-row CT. Eur J Radiol 2004; 52:31–43.
3. Michels NA. Blood supply and anatomy of the upper abdominal organs with a descriptive atlas. Philadelphia: Lippincott, 1955; 139–143.
4. Iezzi R, Cotroneo AR, Giancristofaro D, Santoro M, Storto ML. Multidetector-row CT angiographic imaging of the celiac trunk: anatomy and normal variants. Surg Radiol Anat 2008; 30:303–310.
5. Winston CB, Lee NA, Jarnagin WR, et al. CT angiography for delineation of celiac and superior mesenteric artery variants in patients undergoing hepatobiliary and pancreatic surgery. AJR Am J Roentgenol 2007; 189:13–19.
6. Ilici AT, Kocaoglu M, Bilici A, et al. Median arcuate ligament syndrome: multidetector computed tomography findings. J Comput Assist Tomogr 2007; 31:728–731.
7. Thony F, Baguet JP, Rodiere M, et al. Renal artery entrapment by the diaphragmatic crus. Eur Radiol 2005; 15:1841–1849.
8. Vaziri K, Hungness ES, Pearson EG, Soper NJ. Laparoscopic treatment of celiac artery compression syndrome: case series and review of current treatment modalities. J Gastrointest Surg 2009; 13:293–298.
9. Ikeda O, Tamura Y, Nakasone Y, Yamashita Y. Celiac artery stenosis/occlusion treated by interventional radiology. Eur J Radiol 2009; 71:369–377.
10. Horton KM, Smith C, Fishman EK. MDCT and 3D CT angiography of splanchnic artery aneurysms. AJR Am J Roentgenol 2007; 189:641–647.
11. Knox R, Steinthorsson G, Sumpio B. Celiac artery aneurysms: a case report and review of the literature. Int J Angiol 2000; 9:99–102.
12. Matsukura I, Iwai T, Inoue Y. Celiac artery aneurysm: report of two surgical cases. Surg Today 1999; 29:948–952.
13. Grierson C, Uthappa MC, Uberoi R, Warakaulle D. Multidetector CT appearances of splanchnic arterial pathology. Clin Radiol 2007; 62:717–723.
14. Song SY, Chung JW, Kwon JW, et al. Collateral pathways in patients with celiac axis stenosis: angiographic-spiral CT correlation. Radiographics 2002; 22:881–893.
15. Park CM, Chung JW, Kim HB, Shin SJ, Park JH. Celiac axis stenosis: incidence and etiologies in asymptomatic individuals. Korean J Radiol 2001; 2:8–13.
16. Bron KM, Redman HC. Splanchnic artery stenosis and occlusion: incidence, arteriographic and clinical manifestations. Radiology 1969; 92:323–328.
17. Cademartiri F, Palumbo A, Maffei E, et al. Noninvasive evaluation of the celiac trunk and superior mesenteric artery with multislice CT in patients with chronic mesenteric ischaemia. Radiol Med 2008; 113:1135–1142.
18. Akamatsu N, Sugawara Y, Tamura S, Kaneko J, Togashi J, Makuchi M. Impact of celiac axis stenosis on living donor hepatectomy. Transplant Proc 2006; 38:2948–2950.
19. Okazaki M, Higashihara H, Ono H, et al. Chemoembolization for hepatocellular carcinoma via the inferior pancreaticoduodenal artery in patients with celiac artery stenosis. Acta Radiol 1993; 34:20–25.
20. Lipska L, Visokai V, Levy M, Koznar B, Zaruba P. Celiac axis stenosis and lethal liver ischemia after pancreaticoduodenectomy. Hepatogastroenterology 2009; 56:1203–1206.
21. Smith CL, Horton KM, Fishman EK. Mesenteric CT angiography: a discussion of techniques and selected applications. Tech Vasc Interv Radiol 2006; 9:150–155.